Research Article

Cancer Prevention Research

Metformin Accumulation Correlates with Organic Cation Transporter 2 Protein Expression and Predicts Mammary Tumor Regression *In Vivo*

L. Allyson Checkley[1], Michael C. Rudolph[1], Elizabeth A. Wellberg[2], Erin D. Giles[3], Reema S. Wahdan-Alaswad[2], Julie A. Houck[1], Susan M. Edgerton[2], Ann D. Thor[2], Pepper Schedin[4,5], Steven M. Anderson[2], and Paul S. MacLean[1,2,6]

Abstract

Several epidemiologic studies have associated metformin treatment with a reduction in breast cancer incidence in prediabetic and type II diabetic populations. Uncertainty exists regarding which patient populations and/or tumor subtypes will benefit from metformin treatment, and most preclinical *in vivo* studies have given little attention to the cellular pharmacology of intratumoral metformin uptake. Epidemiologic reports consistently link western-style high fat diets (HFD), which drive overweight and obesity, with increased risk of breast cancer. We used a rat model of HFD-induced overweight and mammary carcinogenesis to define intratumoral factors that confer metformin sensitivity. Mammary tumors were initiated with 1-methyl-1-nitrosourea, and rats were randomized into metformin-treated (2 mg/mL drinking water) or control groups (water only) for 8 weeks. Two-thirds of existing mammary tumors responded to metformin treatment with decreased tumor volumes ($P < 0.05$), reduced proliferative index ($P < 0.01$), and activated AMPK ($P < 0.05$). Highly responsive tumors accumulated 3-fold greater metformin amounts ($P < 0.05$) that were positively correlated with organic cation transporter-2 (OCT2) protein expression ($r = 0.57$; $P = 0.038$). Importantly, intratumoral metformin concentration negatively associated with tumor volume ($P = 0.03$), and each 10 pmol increase in intratumoral metformin predicted >0.11 cm^3 reduction in tumor volume. Metformin treatment also decreased proinflammatory arachidonic acid >1.5-fold in responsive tumors ($P = 0.023$). Collectively, these preclinical data provide evidence for a direct effect of metformin *in vivo* and suggest that OCT2 expression may predict metformin uptake and tumor response. *Cancer Prev Res; 10(3); 198–207. ©2017 AACR.*

Introduction

Metformin is a widely prescribed oral drug given to patients with pre- or frank type II diabetes. Its use has been associated with a decreased incidence and improved outcomes for patients with a variety of cancers, including breast cancer. Epidemiologic studies consistently suggest an anticancer effect of metformin in individuals with diabetes, including breast cancer (1–3). A number of preclinical studies of mammary carcinogenesis and *in vitro* studies using breast cancer cell lines are consistent with this assertion of metformin's beneficial effects (4–9). Even so, other preclinical studies of mammary carcinogenic models failed to see any effect of metformin when the animals were fed a low fat diet and exhibited no metabolic dysfunction (10, 11). These conflicting reports suggest that there may be specific factors and metabolic conditions that confer a tumor's sensitivity to metformin. The importance of understanding metformin's effects in breast cancer and the mechanisms conferring sensitivity to its actions is underscored by the randomized clinical trials currently underway.

Although the putative effects of metformin have not been well understood, it has the potential to affect tumors through direct (cell autonomous) and indirect (systemic) mechanisms. The fact that metformin had little to no effect in preclinical studies in nondiabetic animals on a low fat diet would suggest the systemic effects of metformin are relevant (10, 11). Observations that the effects of metformin are evident or more pronounced in obese or high fat–fed models (12, 13) would support this notion. Even so, numerous studies in breast cancer cell lines have shown that metformin directly affects growth and proliferation through inhibition of mTORC1 in both AMPK-dependent (8) and -independent (14) processes. Additional mechanistic observations using triple-negative breast cancer cell lines implicate inhibition of Stat3 with subsequent growth inhibition and apoptosis induction (8), as well as inhibition of TGFβ-mediated activation of Smad2, Smad3, and ID1 (9). Preclinical rodent studies showing an effect of metformin support these putative direct effects, with AMPK activation and subsequent inhibition of mTORC1 and/or acetyl

[1]Division of Endocrinology, Metabolism and Diabetes, University of Colorado Denver Anschutz Medical Campus, Aurora, Colorado. [2]Department of Pathology, University of Colorado Denver Anschutz Medical Campus, Aurora, Colorado. [3]Department of Nutrition and Food Science, Texas A&M University, College Station, Texas. [4]Department of Cell, Developmental and Cancer Biology, Oregon Health & Science University, Portland, Oregon. [5]Knight Cancer Institute, Oregon Health & Science University, Portland, Oregon. [6]Center for Human Nutrition, University of Colorado Denver Anschutz Medical Campus, Aurora, Colorado.

Note: Supplementary data for this article are available at Cancer Prevention Research Online (http://cancerprevres.aacrjournals.org/).

L.A. Checkley and M.C. Rudolph contributed equally to this article.

Corresponding Author: Paul S. MacLean, University of Colorado, Mail Stop: F-8305: RC1 North 12800 East 19th Avenue, Aurora, CO 80045. Phone: 303-724-3030; Fax: 303-724-3031; E-mail: paul.maclean@ucdenver.edu

doi: 10.1158/1940-6207.CAPR-16-0211-T

CoA carboxylase (ACC) (12, 15). In order to maximize the therapeutic value of metformin, it is important to clarify whether metformin is acting directly or indirectly on tumors.

The direct effect of metformin requires active transport across the cellular membrane. Members of the organic cation transporter (OCT) family, including OCTs 1, 2, and 3, facilitate active cellular uptake of metformin (16). It remains unclear whether tumors express any or all of the OCTs. Zhu and colleagues reported the limited potential of low doses of metformin for prevention and control of N-methyl-N-nitrosourea (MNU)-induced mammary carcinogenesis, which they partially attributed to low gene expression of OCT1 and OCT3 in mammary carcinomas (17). In addition, a neoadjuvant, single-arm, "window of opportunity" trial with metformin, in nondiabetic breast cancer patients, found that all tumors were positive for OCT1 (18). Neither of these studies linked OCT expression to metformin accumulation in tumor tissue, and demonstration of metformin uptake and accumulation in tumors, at levels sufficient to mediate a direct effect *in vivo*, is limited. Supporting the potential for metformin accumulation in tumor tissue, Liu and colleagues recently reported concentrations of metformin reaching micromolar values in ovarian tumor biopsies from patients taking metformin prior to surgery (19).

The purpose of this study was to seek evidence of metformin's direct effect by assessing its accumulation in tumors *in vivo* at physiologically relevant doses. We hypothesized that metformin would decrease tumor volume by targeting tumor cells directly and that the degree of efficacy would be dependent on intratumoral metformin accumulation. We sought evidence for this direct effect using a rat model of mammary carcinogenesis and a standardized high fat diet (HFD) that induced an overweight phenotype. Our observations suggest that metformin accumulates in mammary tumors *in vivo* in relation to OCT2 expression and may prove to be a biomarker predicting tumor uptake and response to metformin treatment.

Materials and Methods

Animals

The animals from this study were selected from a larger parent study focused on the effects of obesity. Female Wistar rats 5 weeks of age (115 ± 1.0 g) purchased from Charles River Laboratories were individually housed in metabolic caging at 22°C to 24°C and 12:12-hour light-dark cycle, provided free access to water, and were placed on purified HFD (46% kcal fat; Research Diets, RD#D12344). In this outbred strain, the response to the HFD is variable. Rats were ranked by percent body fat at 14 to 18 weeks of age as previously described (4). Rats from the middle tertile, that is, rats that displayed moderate weight gain when administered a HFD, were placed on study. All animal procedures were approved by the Institutional Animal Care and Use Committee.

1-Methyl-1-nitrosourea–induced rat mammary carcinogenesis model and study design

At 52 days of age female, Wistar rats described above were given a carcinogenic dose (60 mg/kg) of MNU to induce mammary tumor formation, as previously described (20), to test the *in vivo* effects of metformin treatment on mammary tumor development in the context of a HFD and elevated weight gain. MNU was purchased from MRI Global Chemical Carcinogen Repository. Tumors were detected by manual palpation and measured in three dimensions using digital calipers at weekly intervals from the time of MNU administration. When total tumor volume per rat reached $\geq 1.0\ cm^3$, the rat was randomized to either metformin treatment [2 mg/mL metformin in the drinking water (approximately 70 mg/kg body weight per day); $n = 12$] or a control group (water only; $n = 11$) until time of euthanasia. There was no difference in average time to randomization between groups (Control: 20.8 ± 2.0; Metformin: 20.3 ± 2.5, weeks). There were also no differences in tumor multiplicity (Control: 3.1 ± 0.4; Metformin: 3.2 ± 0.4), total burden (Control: 2.1 ± 0.5; Metformin: 2.5 ± 0.4), or average burden (Control: 0.7 ± 0.1; Metformin: 1.0 ± 0.2). Body weight was monitored weekly. Treatment continued for 8 weeks, at which time animals were euthanized and mammary tumors excised, weighed, and processed for histologic and biochemical evaluation. Tumors were classified as either responders (regressed) if there was a net reduction in tumor volume over the 8-week treatment phase or nonresponders (progressed) if there was a net increase in tumor volume.

Blood collection and plasma biomarker analyses

Blood was collected via venipuncture at time of euthanasia during the latter part of the light cycle, and plasma was isolated and stored at −80°C. Insulin was measured using the Rat Insulin ELISA (ALPCO, 80-INSRT-E01). Leptin was measured using the Mouse/Rat Leptin ELISA (ALPCO, 22-LEPMS-E01). Colorimetric assays were used to measure free fatty acids (FA; Wako Chemicals), glucose, triglycerides, and total cholesterol (#TR15421, TR22321, and TR13521, respectively; Thermo-Fisher).

In vivo body composition

Body composition was determined at the study start for tertile separation and at the time of euthanasia by quantitative magnetic resonance (qMR; Echo MRI Whole Body Composition Analyzer; Echo Medical Systems). Percent liver fat was determined via qMR at time of euthanasia and confirmed via measurement of total liver triglyceride content via the Triglyceride Colorimetric Assay Kit (#10010303; Cayman Chemical).

Immunohistochemistry and quantitative analysis

At euthanasia, mammary tumors were removed from rats and fixed in 10% neutral-buffered formalin, embedded, and sectioned (4 μm). Sections were stained with hematoxylin and eosin for classification, and only adenocarcinomas were included in subsequent analyses. Immunohistochemistry (IHC) images were acquired via the Aperio Digital Pathology Slide Scanner (Leica Biosystems) and quantitatively analyzed via Aperio ImageScope.

Ki-67

Antigen retrieval was performed using 1X Dako TRS Antigen Retrieval Solution (Dako; #S169984) at 125°C under pressure for 10 minutes. Sections were blocked with 3% H_2O_2 (diluted in methanol) for 10 minutes followed by Dako Protein Block (#X0909) for 10 minutes. Sections were then incubated with primary antibody Ki-67 (Thermo Scientific; #RM-9106-S, 1:400) at room temperature for 60 minutes followed by secondary antibody (Dako Envision+ anti-rabbit; #K4003) for 30 minutes. Sections were then incubated with the chromogen 3,3′-diaminobenzidine (Dako; # K346811) for 10 minutes at room temperature and counterstained with hematoxylin for 8 minutes.

OCT2 (*SLC22A2*)

Sections were incubated in 3% H_2O_2 (diluted in methanol) for 10 minutes. Antigen retrieval was performed using Citrate buffer (10 mmol/L; pH 6.0) microwaved on high setting for 2 minutes followed by 15 minutes on low setting. Sections were blocked in normal goat serum diluted in PBS for 15 minutes at room temperature. Sections were then incubated with primary antibody OCT2 (Sigma-Aldrich; #HPA008567, 1:750) overnight at 4°C in a humidity chamber followed by secondary antibody (biotinylated goat anti-rabbit diluted in PBS/BSA, 1:500) for 30 minutes at room temperature. Sections were then incubated with VECTASTAIN Elite ABC (Vector Laboratories; #PK-6100) diluted in PBS/BSA for 30 minutes at room temperature followed by incubation with chromogen 3,3′-diaminobenzidine (Dako; #K346811) for 10 minutes at room temperature and counterstained with Harris Hematoxylin for 60 seconds.

CD68

Sections were incubated in 3% H_2O_2 (diluted in methanol) for 10 minutes. Antigen retrieval was performed using 1X Dako TRS Antigen Retrieval Solution (Dako; #S16998) at 125°C under pressure for 10 minutes. Sections were blocked in 10% normal horse serum diluted in TBS with 1% BSA for 15 minutes at room temperature. Sections were then incubated with primary antibody CD68 (AbD-Serotec; #MCA341; 1:20,000) overnight at 4°C in a humidity chamber followed by secondary antibody (biotinylated horse anti-mouse, rat pre-absorbed, 1:500 with 1% BSA) for 30 minutes at room temperature. Sections were then incubated with VECTASTAIN Elite ABC (Vector Laboratories; #PK-6100) diluted in TBS/BSA for 30 minutes at room temperature followed by incubation with chromogen 3,3′-diaminobenzidine (Dako; #K346811) for 10 minutes at room temperature and counterstained with Harris Hematoxylin for 60 seconds.

Western blotting

Tumors were pulverized in liquid nitrogen, lysed in Mammary Lysis Buffer (50 mmol/L Tris, pH 7.4, 150 mmol/L NaCl, 2 mmol/L EDTA, 50 mmol/L NaF, 1% Triton X-100, 1% sodium deoxycholate, 0.1% SDS, 5 mmol/L sodium vanadate), and supplemented with Halt Protease and Phosphatase Inhibitor cocktail (Thermo Scientific; # 1861281). Protein levels were determined by capillary electrophoresis size-based separating via the WES from ProteinSimple according to the manufacturer's instructions. Data were analyzed with Compass software (ProteinSimple). Primary antibodies used were Acetyl-CoA Carboxylase 1 (ACC1; Cell Signaling Technology; #4190, 1:200), p-Acetyl-CoA Carboxylase (Ser79; Cell Signaling Technology; #3661, 1:200), AMP-activated protein kinase alpha (AMPKα; Cell Signaling Technology; #2532, 1:50), and p-AMPK–activated protein kinase alpha (Thr 172; Cell Signaling Technology; #2535, 1:50). All proteins were normalized to β-actin or vinculin (Cell Signaling Technology, #4970, 1:300; Sigma Aldrich, #V9131, 1:50,000, respectively). Electropherograms are represented in Supplementary Fig. S3.

Gas chromatography-mass spectrometry

Metformin quantification. High Performance Liquid Chromatography (HPLC) grade reagents were used for all gas chromatography-mass spectrometry (GC/MS) preparations (Sigma Aldrich). Ten to 40 mg of snap-frozen pulverized tumor or liver was added directly to 500 μL of 100 mmol/L potassium phosphate buffer pH 7.2, and samples were homogenized mechanically until uniform. Two hundred fifty microliter of lysate was snap-frozen for later FA profiling (see below), and 15 ng of stable isotope [D_6]-metformin reference standard (ALSACHIM) was added to the remaining 250 μL and vortexed. For plasma, 25 μL of thawed plasma was added directly to 250 μL of 100 mmol/L potassium phosphate buffer pH 7.2, 15 ng of [D_6]-metformin was added, and samples were vortexed. Note that 1 mL of 10 mol/L NaOH was added, samples were vortexed vigorously, 6 mL of 1-chlorobutane was added, and samples were shaken vigorously for 30 seconds. Samples were rotated at 27°C for 10 minutes, after which they were centrifuged at 300 x *g* for 10 minutes. Top organic phase was collected into new tubes, and metformin was derivatized by addition of 50 μL of tertafluoroacetic anhydride at 45°C for 45 minutes, after which samples were taken to dryness under gaseous nitrogen. Samples were reconstituted in 100 μL of acetonitrile, and 1 μL was injected for GC/MS analysis. A calibration curve was generated using 130, 65, 32.5, 16.25, 8.12, 4.06, and 2.0 ng metformin (analyte) relative to 25 ng [D_6]-metformin (standard). *In vivo* quantities of metformin were determined by the peak area ratio relative to the internal stable isotope standard peak area divided by the calibration curve slope.

Lipid mass spectrometry. Tumor FA profiles were extracted and quantified by GC/MS as previously described (21, 22), and are expressed in nmoles of FA per mg of tumor protein. The total n-6/n-3 FA ratio is the quantitative sum of n-6 (18:2, 18:3, 20:2, 20:3, 20:4, 22:2, 22:4, and 22:5) divided by the sum of n-3 (18:3, 20:3, 20:4, 20:5, 22:3, 22:5, and 22:6); the AA/DHA ratio is the absolute amount of 20:4 n-6 divided by 22:6 n-3; the LA/LNA ratio is the absolute amount of 18:2 n-6 divided by 18:3 n-3.

Statistical analysis

A two-way ANOVA was utilized to compare average number of regressed, progressed, and new tumors in each treatment group as well as changes in tumor volume. To compare OCT2 positivity, Ki67 positivity, and metformin accumulation between responders and nonresponders, data were presented as the mean ± the SEM and were analyzed using a two-tailed *T* Test. Spearman's correlation coefficient was used to calculate the correlation coefficient (one-tailed) for percent OCT2 positivity and metformin accumulation. Differences in metformin accumulation between tumors, livers, and plasmas were analyzed with a one-way ANOVA. Statistical significance was assumed with a *P* value of 0.05 or lower for all tests. These statistical tests were completed with GraphPad Prism 7 software (GraphPad Software). For multivariable linear regression, the primary outcome was the change in tumor volume, and either metformin retention or the AA:DHA ratio was the predictor. Covariates considered in the models were Ki67 proliferative index and duration of metformin treatment. Multivariable linear regression analyses were conducted in JMP Pro, Version 12.1.0 (SAS Institute Inc., 1989-2007).

Results

Metformin inhibits mammary tumor progression and proliferation

In order to directly test the *in vivo* effects of metformin on mammary tumor development and progression, rats were placed on HFD, and carcinogenesis was initiated (Fig. 1). Following

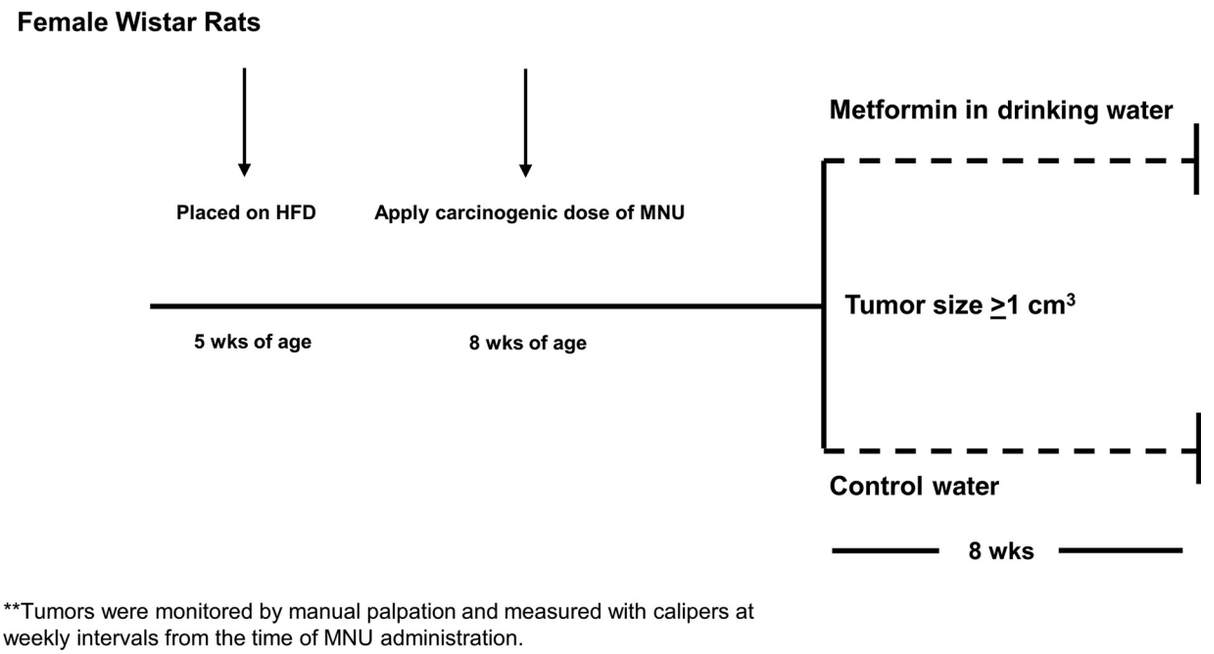

Figure 1.

Design to investigate the effect of metformin on mammary tumor progression. Female Wistar rats were placed on HFD (46%) at 5 weeks of age followed by MNU administration (60 mg/kg) at 8 weeks of age. Once tumor burden reached ≥ 1 cm^3, rats were randomized into a control or metformin (2 mg/mL in drinking water) group for the 8-week study duration.

8 weeks of treatment, 65% of existing mammary tumors in the metformin-treated group regressed (decreased in tumor volume) compared with only 24% in the control group, a 2.7-fold increase ($P < 0.05$) relative to the untreated group (Fig. 2A). Conversely, the metformin-treated group had a 2-fold reduction in the number of progressed tumors, whereas the number of new tumors appearing between groups was not different (Fig. 2A). These data are presented in Fig. 2A as the average number of tumors per animal that either progressed, regressed, or newly developed. This equated to 1.67 ± 0.31(metformin) versus 0.64 ± 0.15 (control) tumors per rat that regressed and 0.92 ± 0.29 (metformin) versus 2.00 ± 0.47 (control) that progressed at study conclusion. Tumor volume tended to be lower in the metformin-treated group which was presented as the average percent change in volume, and means were statistically significant at weeks 5, 6, 7, and 8 (Fig. 2B; $P < 0.05$). Although not statistically significant, metformin-treated rats tended to have a higher study completion percentage relative to controls (72.7% vs. 45.5%; Fig. 2C) as almost half of the control animals' tumor burden reached the ethical limitations and could not be continued on study. Metformin-treated mammary tumors displayed a lower Ki-67 proliferative index compared with the control tumors (Fig. 2D and E). The lower number of proliferating tumor cells was concomitant with an increase in total AMPK levels, although the phosphorylated AMPK and fraction of phosphorylated to total AMPK were unchanged (Fig. 2F and G). Phosphorylation of the AMPK target enzyme ACC at inhibitory site Ser79 was significantly greater in metformin-treated tumors, as was the fraction of inhibited to total ACC (Fig. 2F and G; $P < 0.01$ and 0.05, respectively).

Body morphometry and metabolic status were unchanged following metformin intervention

Body composition and fat accumulation in the liver were measured by qMR at the time of euthanasia (Table 1A). No differences were observed between control and metformin-treated groups for total body mass or for percent body fat (Table 1A). Similarly, metformin treatment did not affect total liver weight when compared with controls nor did it alter total liver fat accumulation or total liver TG (nmol/mg; Table 1A). Systemic markers of metabolic health were also evaluated, as metformin is regularly prescribed to improve whole body metabolism in patients with Type II Diabetes. Circulating levels of insulin, glucose, leptin, TG, cholesterol, and non-esterified FA were unchanged between treatment groups (Table 1B). Metformin treatment in HFD-fed rats had no substantial effect on the selected whole body metrics of metabolic health that were quantified. Although these data do not rule out systemic effects of metformin, they suggest that the beneficial effects of metformin in our study were not likely due to dramatic improvements in whole body metabolism.

Metformin accumulates in mammary tumors and amounts predict treatment response

To determine whether the observed effects of metformin upon tumor-bearing rats occurred at concentrations that are considered clinically relevant in humans, metformin levels in tumors, plasma, and livers of metformin-treated rats were quantified using GC/MS. Plasma levels of metformin in all treated animals were within the range considered to be physiological in humans (0.7–1.5 mg/L, not shown; refs. 23, 24). A marked accumulation of metformin was observed in tumors relative to the plasma of the

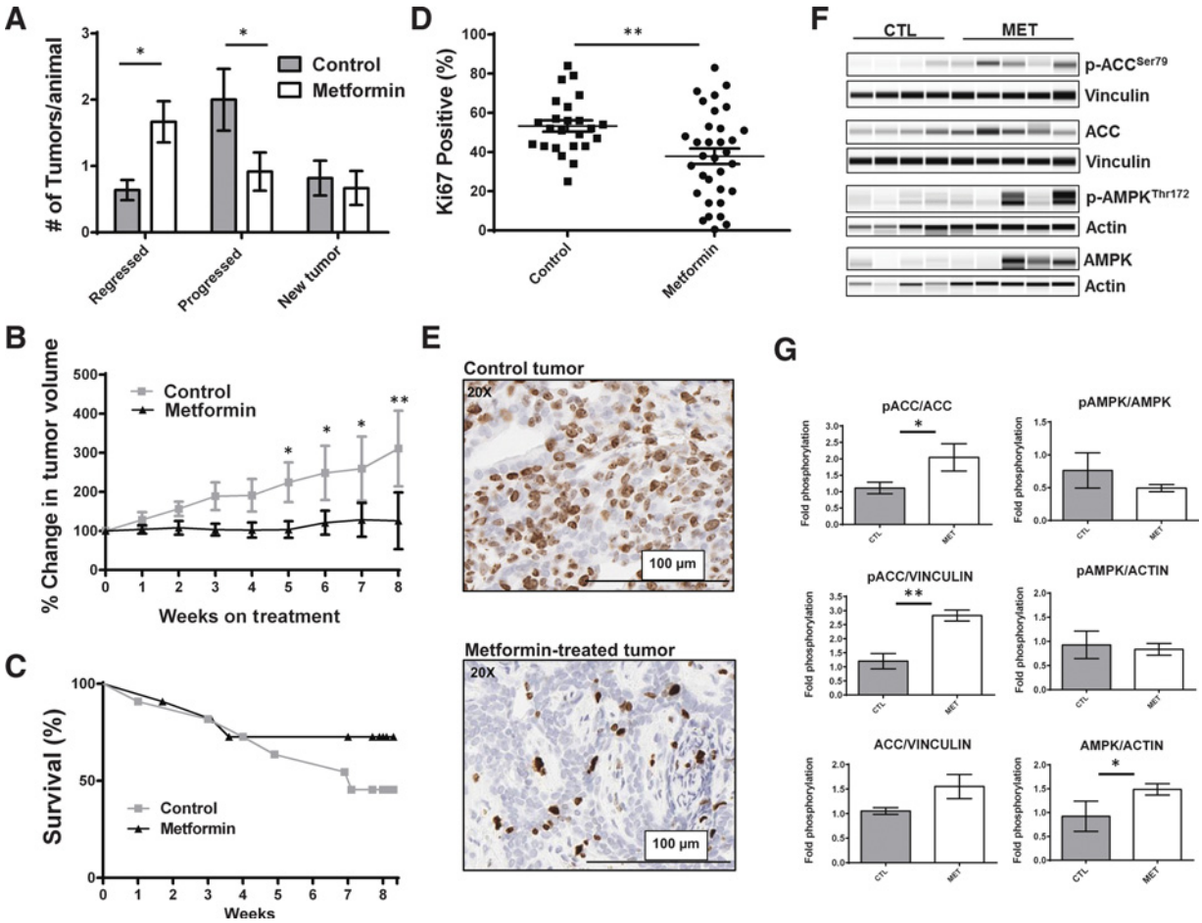

Figure 2.

Effect of metformin on mammary tumor development and progression. **A,** Average number of tumors that regressed, progressed, or newly developed at the end of 8 weeks. Sixty-five percent of tumors regressed within the metformin-treated group versus 24% in the control group (Con tumors, $n = 38$; Met tumors, $n = 39$; *, $P < 0.05$). There was no significant difference in new tumor development between groups. Data are presented as average number of tumors per animal that regressed, progressed, or newly developed at study conclusion. **B,** Percent change in overall tumor volume throughout the course of the study; weeks 5, 6, 7, and 8 were significantly different between groups ($P = 0.02$–0.007). **C,** Survival curves for control and metformin-treated groups for study duration (Con animals, $n = 11$; Met animals, $n = 12$). **D,** Cellular proliferation in metformin-treated mammary tumors compared with control mammary tumors as determined by positive staining via proliferative marker Ki67 (Con tumors, $n = 28$; Met tumors, $n = 34$;**, $P < 0.01$). **E,** Representative images of Ki-67 staining are shown from a control and metformin-treated mammary tumor (responder, low Ki67; 20x). **F,** Representative images of p-ACC^{Ser79}, ACC, pAMPK^{Thr172}, and AMPK in whole cell tumor lysates (WES ProteinSimple). **G,** Quantitation of western blots (Con tumors, $n = 4$; Met tumors, $n = 5$; *, $P < 0.05$; **, $P < 0.01$).

same animal [45 parts per billion (ppb) vs. 6.8 ppb; $P < 0.01$; Fig. 3A]. Accumulation of metformin was increased in the tumor compared with that observed in the liver, although the difference was not statistically significant. Importantly, the amount of metformin retained by the tumor was significantly associated with the observed reduction in tumor volume ($P = 0.03$), and the amount of metformin present predicted the decrease in tumor volume (Fig. 3B). The multivariable regression model predicts that for each 10 pmol/L increase in intratumoral metformin amount, tumor volume should decrease approximately 0.110 cm^3 ($\beta = -0.011$ cm^3 per 1.0 pmol/L metformin). Furthermore, when tumors in the metformin-treated group were classified as responders (regressing) or nonresponders (progressing), the responders had significantly greater metformin accumulation as compared with the nonresponders ($P < 0.05$; Fig. 3C).

OCT2 mediates antitumor efficacy of metformin in mammary tumors

Given the potential direct effects of metformin on the proliferative potential of mammary tumors *in vivo*, expression of a representative metformin transporter was examined. Mammary tumor protein expression of OCT2, a dominant regulator of metformin pharmacokinetics (25), was quantified in mammary tumors via IHC staining. Metformin treatment did not alter cell membrane levels of OCT2 compared with control tumors (Fig. 4A); however, within the metformin-treated group, tumors responding to metformin had a greater percentage of cells that stained positive for OCT2 ($P < 0.001$) relative to the nonresponding tumors (Fig. 4B). Importantly, the intratumoral amount of metformin correlated with OCT2 levels within the same tumor ($r = 0.565$; $P = 0.038$; Fig. 4C). Further, within the metformin treatment group, tumors that responded to

Table 1. Physiologic and plasma characteristics of control and metformin-treated tumor-bearing rats at study conclusion. **A,** Body and liver composition were determined using qMR. Triglyceride liver content was measured via colorimetric assay ($n = 8$–11). **B,** Plasma isolated from blood samples obtained via venipuncture in the vena cava at sacrifice was used to measure metabolic markers in the blood ($n = 9$–10)

A

Physiologic characteristics at time of sacrifice

	Control	Metformin
Body weight (g)	323 ± 28	332 ± 20
Body fat (%)	22.4 ± 1.9	22.6 ± 1.8
Liver weight (g)	10.5 ± 1.3	10.1 ± 0.7
Liver fat (%)	6.5 ± 0.8	7.1 ± 0.9
Liver TG (nmoles/mg)	0.38 ± 0.04	0.36 ± 0.03

B

Plasma characteristics at time of sacrifice

	Control	Metformin
Glucose (mmol/L)	9.3 ± 0.8	11.5 ± 0.7
Insulin (pmol/L)	55.9 ± 17.7	45.4 ± 4.7
Leptin (μg/mL)	2.0 ± 0.6	2.4 ± 0.7
TG (mmol/L)	0.53 ± 0.1	0.53 ± 0.1
NEFA (μmol/L)	798 ± 64	856 ± 126
Cholesterol (mmol/L)	1.3 ± 0.3	1.4 ± 0.2

metformin treatment had greater membrane localization of OCT2 compared with nonresponding tumors (Fig. 4D, representative sections). These results implicate OCT2 expression as a critical mediator of cellular metformin uptake in mammary tumors and suggest that low or no expression could significantly impair or prevent the anticancer activity of metformin on neoplastic tissue.

Intratumoral metformin accumulation and reduced tumor volume coincide with decreased proinflammatory FA

Although numerous mechanisms of metformin action have been reported in breast cancer studies, emerging evidence indicates negative regulation of tumor lipid metabolism and phospholipid remodeling with AMPK as the molecular transducer (reviewed in 26). Given our findings of reduced proliferation, elevated phosphorylation of ACC (inhibitory Ser79; Fig. 2), and OCT2-associated metformin accumulation in responsive tumors (Fig. 4), we tested the hypothesis that greater levels of intratumoral metformin accumulation would inhibit lipid metabolism. Within the metformin-treated tumors stratified by progression status, responsive tumors had a 1.51-fold decrease in arachidonic acid (20:4 n-6, AA; $P = 0.023$) with a reciprocal 1.73-fold increase in linolenic acid (LNA, 18:3 n-3; $P = 0.003$). Although the majority of individual FA were not significantly different between responders and nonresponders (Supplementary Table S1), the relative amounts of various n-6 to n-3 FA were significantly lower in metformin-treated responsive tumors (Fig. 5A). The total n-6/n-3, the AA/DHA, and the LA/LNA FA ratios were lower in metformin-responsive mammary tumors by 1.35-fold ($P = 0.002$), 1.26-fold ($P = 0.007$), and 1.47-fold ($P = 0.028$), respectively. Within metformin-treated tumors, the AA/DHA ratio significantly predicted a 0.125 cm^3 increase in tumor volume ($P = 0.013$), when controlling for metformin accumulation, tumor proliferation, and treatment duration (Fig. 5B). Together, a greater concentration of intratumoral metformin accumulated in responsive tumors (Fig. 3C) and coincided with a decreased proinflammatory n-6/n-3 FA ratio (Fig. 5A), and the greater the AA/DHA ratio the greater the tumor volume (Fig. 5B).

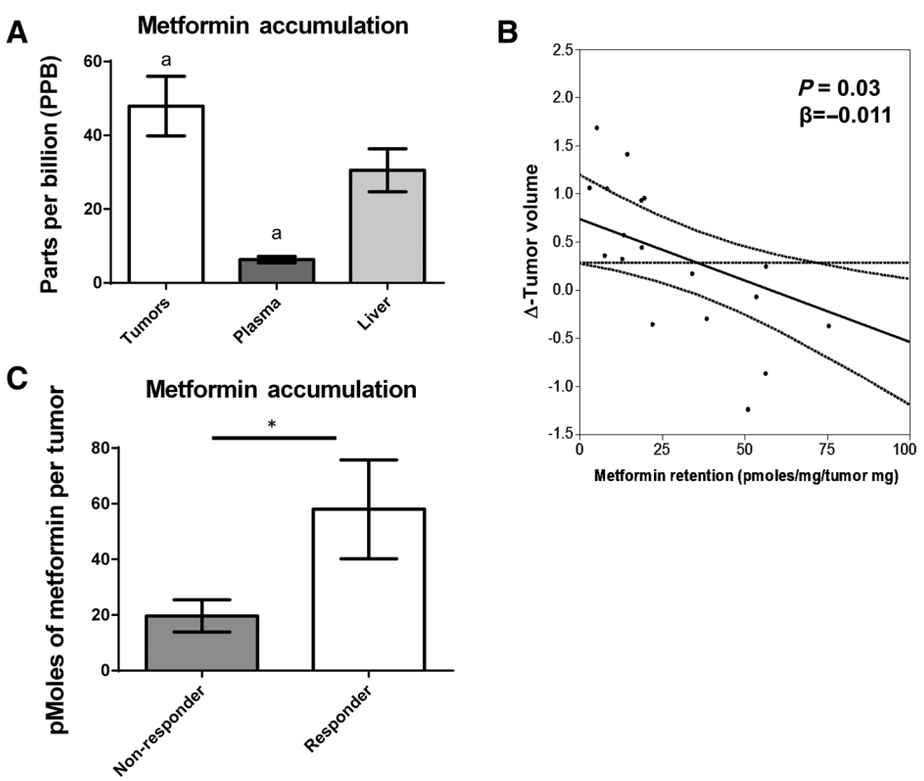

Figure 3.
Metformin accumulates in mammary tumor tissue. **A,** Metformin accumulation was measured via mass spectrometry in a subset of tumors and corresponding livers and plasmas. Metformin accumulation (concentration) was significantly higher in tumor tissue compared with circulating plasma. Data are represented in ppb for tissue comparison. Groups designated by a are significantly different from one another ($P < 0.01$; liver, plasma, $n = 8$; tumors, $n = 19$). **B,** Multivariable linear regression for the significant association between metformin retention and the change in tumor volume, controlling for duration of metformin treatment and tumor cell proliferation (Ki67 positivity; $n = 18$). **C,** Metformin concentration represented as pmoles/tumor was significantly higher in responders compared to nonresponders (*, $P < 0.05$; responders: $n = 8$; nonresponders: $n = 11$).

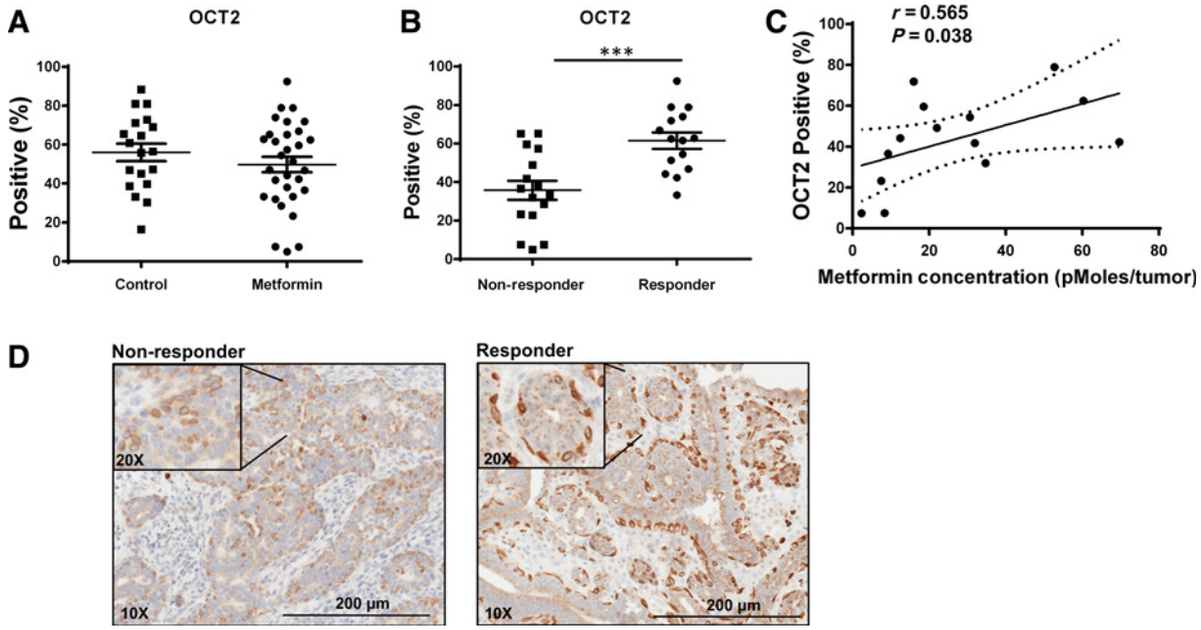

Figure 4.

Metformin uptake and accumulation is mediated by expression of OCT2. **A,** Metformin (●) did not significantly alter expression levels of OCT2 compared with untreated control tumors (■) (Con, $n = 19$, Met, $n = 31$; $P = 0.31$). **B,** A higher percentage of total OCT2-positive tumor cell membranes was detected in responders (●) compared with nonresponders (includes progressing and new tumors) (■) (Res, $n = 15$, Non-res, $n = 16$; ***, $P < 0.0001$). **C,** Moderate positive correlation between OCT2 membrane expression and metformin concentration as measured by mass spectrometry ($n = 14$, Spearman's coefficient, $r = 0.565$, $P = 0.038$). **D,** Representative immunostaining of tumor sections from both responding and nonresponding metformin-treated tumors.

Discussion

The potential effectiveness for breast cancer therapy, as well as the precise patient populations that will benefit most from metformin treatment, remains unclear, because few studies have investigated accumulation of the drug in tumors. To directly address this gap, we quantified metformin amounts in mammary tumors using GC/MS. Plasma levels of metformin achieved in tumor-bearing rats maintained on HFD in this study are consistent with plasma levels well tolerated in humans (Fig. 3; refs. 23, 24). Our primary finding that *in vivo* metformin amounts in tumors were 6-fold higher than in the corresponding plasma indicates mammary tumors accumulate the drug. Most significantly, when tumors were stratified by their decrease in volume, intratumoral metformin amounts were significantly higher in responsive tumors than in nonresponsive ones. We found tumor metformin accumulation is related to tumor volume reduction, in that, multivariable linear regression indicates the decreasing tumor volume is strongly predicted by the increasing amount of intratumoral metformin accumulation, when controlling for length of treatment and tumor proliferation. Metformin

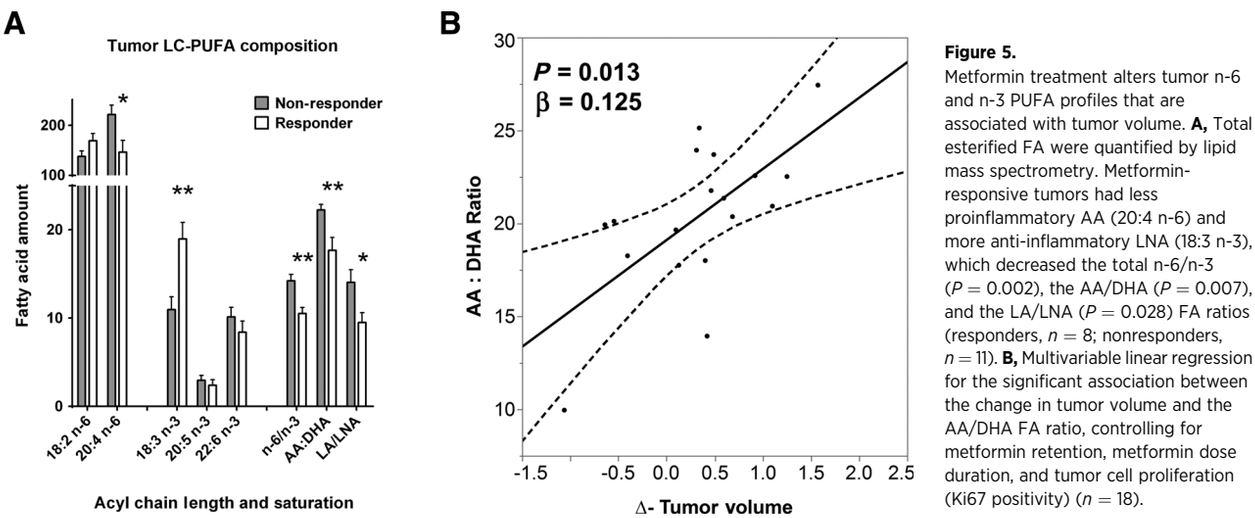

Figure 5.

Metformin treatment alters tumor n-6 and n-3 PUFA profiles that are associated with tumor volume. **A,** Total esterified FA were quantified by lipid mass spectrometry. Metformin-responsive tumors had less proinflammatory AA (20:4 n-6) and more anti-inflammatory LNA (18:3 n-3), which decreased the total n-6/n-3 ($P = 0.002$), the AA/DHA ($P = 0.007$), and the LA/LNA ($P = 0.028$) FA ratios (responders, $n = 8$; nonresponders, $n = 11$). **B,** Multivariable linear regression for the significant association between the change in tumor volume and the AA/DHA FA ratio, controlling for metformin retention, metformin dose duration, and tumor cell proliferation (Ki67 positivity) ($n = 18$).

treatment resulted in a reduction in mammary tumor proliferation, with fewer progressing and more regressing tumors. Together, these results support that, in a model of HFD-induced overweight and mammary carcinogenesis, metformin-responsive mammary tumors accumulate more drug than nonresponsive tumors at physiologically relevant plasma concentrations.

Numerous preclinical *in vivo* (4, 6, 12, 27, 28) and *in vitro* (5, 7–9, 14, 29) cancer models have provided evidence of metformin's antitumorigenic potential, which is commonly attributed to indirect whole-body effects (insulin-dependent) and/or direct (insulin-independent) effects (30). Metformin has been shown to reduce hyperinsulinemia and glycemia, thereby reducing tumor cell insulin receptor expression and downstream signaling (30). We investigated the antitumor effects of metformin on mammary tumors in rats fed a HFD. It has been suggested that a HFD with a high n-6 PUFA content may influence the incidence of breast cancer in Western women (31), and lifestyle intervention designed to reduce dietary fat intake may also lower the risk of relapse in woman with early stage, resected breast cancer (32). Compared with standard chow-fed rat models of human obesity and metabolic syndrome (33), animals provided the HFD in this study had approximately 1.5- to 2.2-fold increase in percent body fat, indicating that they were overweight due to increased adiposity. In our study, relative to untreated controls, metformin treatment caused no change in body weight, percent body fat, or plasma concentrations of insulin, leptin, free FA, or liver TG (Table 1 and Supplementary Fig. S1), supporting the hypothesis that metformin can directly affect tumor cell biology in the absence of obvious effects on systemic markers of metabolism. These data provide support for a direct mechanism of metformin action on tumor cells in our model system.

In contrast to our findings, a limited number of rodent studies have suggested that metformin does not affect mammary carcinogenesis (10, 11). However, there are key differences in study design between our study and these previous reports that include variations in rodent age at initiation with MNU, diet, and dosage of metformin. Most notably, both studies reported use of a standard chow diet low in fat in contrast to the HFD incorporated in our study design. It is possible that a low fat diet prevented detection of metformin-mediated anticancer effects.

Cellular metformin uptake requires expression of OCTs such as OCT1, OCT2, and OCT3 to facilitate uptake (16). We found that intratumoral metformin accumulation was highly correlated with OCT2 positivity, and responsive tumors had significantly greater OCT2 protein expression. Furthermore, metformin concentrations were higher in tumor tissue relative to levels measured in the plasma or liver of the same animal. When tumors were classified by changes in volume, responsive tumors had significantly greater OCT2 expression and metformin uptake relative to nonresponding tumors, supporting the relevance of OCT2. To that end, Kimura and colleagues concluded OCT2 had enhanced metformin transport capacity compared with OCT1 (25). It is possible that alternative transporters may also play a role in tumor cell metformin uptake contributing to direct metformin effects *in vivo*. A recent study found overexpressing OCT3 in BT-20 breast cancer cells (triple negative) positively correlated with metformin uptake, increasing metformin uptake >13-fold and decreasing proliferation 4-fold, which established a clear relationship between rate of selective metformin uptake and suppression of breast cancer cell proliferation (34).

Regulation of transporter expression may also play a role in metformin-mediated direct effects on cancer cells. In concordance, hormonal regulation of kidney OCT2 expression was demonstrated in rats; testosterone upregulated OCT2, and estradiol moderately downregulated OCT2 (35). Other studies identified variability in transporter expression profiles among luminal and basal (triple negative) breast cancer cell lines, with some triple-negative lines showing higher levels of transporter expression, suggesting that heterogeneity in breast cancer tissue may also play a role in response to metformin (34). Triple-negative breast cancer cells are more sensitive to metformin as compared with luminal lines (7). Our current study represents a luminal, estrogen receptor–positive (data not shown), model of breast cancer. Future studies will aim at measuring expression levels of transporters in basal mammary tumors, as metformin effectiveness may be dose-dependent on cation-transporter expression. Gene variants of cation transporters may also play a role in determining subpopulation responsiveness to drug treatment in a cancer setting. Genetic polymorphisms in *SLC22A1* (OCT1) and *SLC22A2* (OCT2) are associated with variability in metformin response in diabetics (36). The potential for tumor metformin uptake indicates that transporter evaluation in pretreatment biopsies may identify women most likely to respond.

Direct metformin action inhibits mitochondrial complex I to induce cellular energetic stress and subsequent activation of energy sensor, AMPK (37). Consistent with a direct metformin and AMPK-dependent mechanism, our findings indicate metformin-mediated mammary tumor regression was correlated with a reduced proliferative index (Ki67), increased AMPK activation, and subsequent inhibitory phosphorylation of ACC. Inhibitory serine 79 phosphorylation of ACC, a direct substrate of AMPK, within mammary tumors treated with metformin supports a potential AMPK-dependent mechanism. Activating AMPK by metformin *in vitro* limits lipogenesis via negative regulation of ACC (38) and FAS (7), which is thought to change the FA profile of tumors (39, 40). In mammary tumors that were highly responsive to metformin intervention, the tumor lipid profile was altered. Both n-6 and n-3 series PUFA are critical FA making up the phospholipids in cell membranes, and their incorporation into phospholipids is required by rapidly proliferating breast cancer cells (41, 42). Emerging evidence implicates increased tumor phospholipid remodeling and lipid oxidation as processes influenced by metformin in cancer with AMPK as the molecular sensor (26, 40). Our findings indicate metformin-responsive tumors have reduced total n-6/n-3 FA ratio, driven by a reduction of AA (20:4 n-6) to decrease the AA:DHA ratio, as well as the reciprocal increase of LNA (18:3 n-3) to reduce the LA/LNA ratio, compared with nonresponding tumors.

The ratio of n-6 to n-3 PUFA present in tumors plays a critical role in biophysical organization of membranes and lipid rafts changing oncogenic receptor localization (43–45), enhancing supply of proinflammatory LA and AA for eicosanoid and prostaglandin synthesis (46, 47), and promoting breast cancer cell migration, invasion, and metastasis (44). Recently, dietary fish oil n-3 FA were shown to inhibit mammary tumor progression in obese ovariectomized mice, possibly by lowering adipose inflammation and activating c-JNK to inhibit proliferation and initiate apoptosis (48). We observed no significant difference in intratumoral macrophage recruitment assessed by CD68 IHC scoring, either by metformin treatment relative to control tumors or when grouped by metformin responsiveness (Supplementary Fig. S2).

Our results indicate metformin-responsive mammary tumors have depleted proinflammatory AA, in exchange for LNA reserves, specifically in esterified lipids of the tumor. It is tempting to speculate that intracellular metformin acts on tumor FA metabolism potentially to alleviate proliferative n-6 series ligands (AA or its derivatives), and enrich n-3 series ligands (LNA or its derivatives) that can oppose proliferation. Indeed, dietary n-3 supplementation increased mammary tumor phospholipids containing n-3 PUFA, concomitantly with decreased phospholipid AA, resulting in decreased tumor growth *in vivo* (49). At present, we do not understand if this observation is dependent on HFD consumption, or if metformin might generally affect the balance of n-6 and n-3 FA only in OCT2-positive mammary tumors. Future *in vivo* studies are needed to dissect these metformin treatment effects on the phospholipid landscape, and its FA composition, as a means to identify breast cancer–afflicted women with a greater likelihood of response.

Preclinical models of mammary carcinogenesis (4, 6) and neoadjuvant "window of opportunity" clinical studies (18, 50) have shown the potential utility of metformin for the prevention and/or therapy of breast cancer. However, discrepancies in preclinical results and a lack of pharmacologic studies and identification of biomarkers relative to metformin's anticancer efficacy have prevented determination of the subpopulations and/or cancer types that will benefit most. The *in vivo* findings of tumor-specific expression of critical metformin uptake transporter OCT2, coupled with the demonstration of tumor-specific metformin accumulation, provide compelling evidence for a direct metformin-mediated effect in breast cancers irrespective of host metabolic status. Nonetheless, additional studies are needed to determine the degree to which tumor subtype, adiposity, and metabolic health influence metformin response. Further, it would be interesting to evaluate if metformin intervention, in combination with dietary n-3 FA, could augment existing breast cancer treatment modalities to improve prevention, attenuate progression, and enhance survivorship, especially in postmenopausal women predisposed to weight gain and enhanced breast cancer risk. Collectively, our data fill a gap in preclinical knowledge related to metformin and cancer therapeutics, as most *in vivo* studies to date fail to address pharmacologic parameters and putative biomarkers related to metformin response and may facilitate translation to the clinic.

Disclosure of Potential Conflicts of Interest

No potential conflicts of interest were disclosed.

Authors' Contributions

Conception and design: L.A. Checkley, E.A. Wellberg, E.D. Giles, A.D. Thor, P. Schedin, P.S. MacLean

Development of methodology: L.A. Checkley, M.C. Rudolph, E.A. Wellberg, E.D. Giles, J.A. Houck, A.D. Thor, P.S. MacLean

Acquisition of data (provided animals, acquired and managed patients, provided facilities, etc.): L.A. Checkley, M.C. Rudolph, E.A. Wellberg, E.D. Giles, R.S. Wahdan-Alaswad, J.A. Houck, S.M. Edgerton, P. Schedin, P.S. MacLean

Analysis and interpretation of data (e.g., statistical analysis, biostatistics, computational analysis): L.A. Checkley, M.C. Rudolph, E.A. Wellberg, S.M. Edgerton, A.D. Thor, P. Schedin, P.S. MacLean

Writing, review, and/or revision of the manuscript: L.A. Checkley, M.C. Rudolph, E.A. Wellberg, E.D. Giles, J.A. Houck, S.M. Edgerton, A.D. Thor, P. Schedin, S.M. Anderson, P.S. MacLean

Administrative, technical, or material support (i.e., reporting or organizing data, constructing databases): L.A. Checkley, E.D. Giles, J.A. Houck, A.D. Thor, S.M. Anderson, P.S. MacLean

Study supervision: L.A. Checkley, E.D. Giles, P.S. MacLean

Other (assisted with biweekly animal inspections, tumor palpations, and animal weight. Assisted with review of manuscript): R.S. Wahdan-Alaswad

Other (sample processing and optimization of methods): J.A. Houck

Acknowledgments

The authors thank Robera Oljira, Ginger Johnson, and Patricia Webb for their technical assistance. The authors also acknowledge the use of the Research Histology Shared Resource and the Biorepository Shared Resource of the University of Colorado Cancer Center (supported by P30 CA046934).

Grant Support

This study was supported by NIH/NCICA164166 (P.S. Maclean and P. Schedin), NIH5 K12 HD057022 BIRCWH and NORC5P30DK048520-19 Pilot Award (M.C. Rudolph), NIH/NCICA169430 (E.D. Giles), NIH/NICHDP01 HD 038129 (S.M. Anderson and P.S. Maclean), and the Cancer League of Colorado (S.M. Anderson and E.A. Wellberg). Lipid mass spectrometry was supported by NIH/NCATS Colorado CTSA Grant UL1 TR001082. This research also utilized University of Colorado Cancer Center Shared Resources which are supported by P30 CA046934.

The costs of publication of this article were defrayed in part by the payment of page charges. This article must therefore be hereby marked *advertisement* in accordance with 18 U.S.C. Section 1734 solely to indicate this fact.

Received August 16, 2016; revised January 19, 2017; accepted January 20, 2017; published OnlineFirst February 2, 2017.

References

1. Bowker SL, Majumdar SR, Veugelers P, Johnson JA. Increased cancer-related mortality for patients with type 2 diabetes who use sulfonylureas or insulin. Diabetes Care 2006;29:254–8.
2. Decensi A, Puntoni M, Goodwin P, Cazzaniga M, Gennari A, Bonanni B, et al. Metformin and cancer risk in diabetic patients: A systematic review and meta-analysis. Cancer Prev Res (Phila) 2010;3:1451–61.
3. Evans JM, Donnelly LA, Emslie-Smith AM, Alessi DR, Morris AD. Metformin and reduced risk of cancer in diabetic patients. BMJ 2005;330:1304–5.
4. Giles ED, Wellberg EA, Astling DP, Anderson SM, Thor AD, Jindal S, et al. Obesity and overfeeding affecting both tumor and systemic metabolism activates the progesterone receptor to contribute to postmenopausal breast cancer. Cancer Res 2012;72:6490–501.
5. Zakikhani M, Dowling R, Fantus IG, Sonenberg N, Pollak M. Metformin is an AMP kinase-dependent growth inhibitor for breast cancer cells. Cancer Res 2006;66:10269–73.
6. Anisimov VN, Egormin PA, Piskunova TS, Popovich IG, Tyndyk ML, Yurova MN, et al. Metformin extends life span of HER-2/neu transgenic mice and in combination with melatonin inhibits growth of transplantable tumors in vivo. Cell Cycle 2010;9:188–97.
7. Wahdan-Alaswad RS, Cochrane DR, Spoelstra NS, Howe EN, Edgerton SM, Anderson SM, et al. Metformin-induced killing of triple-negative breast cancer cells is mediated by reduction in fatty acid synthase via miRNA-193b. Horm Cancer 2014;5:374–89.
8. Deng XS, Wang S, Deng A, Liu B, Edgerton SM, Lind SE, et al. Metformin targets Stat3 to inhibit cell growth and induce apoptosis in triple-negative breast cancers. Cell Cycle 2012;11:367–76.
9. Wahdan-Alaswad R, Harrell JC, Fan Z, Edgerton SM, Liu B, Thor AD. Metformin attenuates transforming growth factor beta (TGF-beta) mediated oncogenesis in mesenchymal stem-like/claudin-low triple negative breast cancer. Cell Cycle 2016;15:1046–59.
10. Zhu Z, Jiang W, Thompson MD, Echeverria D, McGinley JN, Thompson HJ. Effects of metformin, buformin, and phenformin on the post-initiation stage of chemically induced mammary carcinogenesis in the rat. Cancer Prev Res (Phila) 2015;8:518–27.

11. Thompson MD, Grubbs CJ, Bode AM, Reid JM, McGovern R, Bernard PS, et al. Lack of effect of metformin on mammary carcinogenesis in nondiabetic rat and mouse models. Cancer Prev Res (Phila) 2015;8:231–9.
12. Checkley LA, Rho O, Angel JM, Cho J, Blando J, Beltran L, et al. Metformin inhibits skin tumor promotion in overweight and obese mice. Cancer Prev Res (Phila) 2014;7:54–64.
13. Zhang Q, Celestino J, Schmandt R, McCampbell AS, Urbauer DL, Meyer LA, et al. Chemopreventive effects of metformin on obesity-associated endometrial proliferation. Am J Obstet Gynecol 2013;209:24 e1–24 e12.
14. Kalender A, Selvaraj A, Kim SY, Gulati P, Brule S, Viollet B, et al. Metformin, independent of AMPK, inhibits mTORC1 in a rag GTPase-dependent manner. Cell Metab 2010;11:390–401.
15. Tomimoto A, Endo H, Sugiyama M, Fujisawa T, Hosono K, Takahashi H, et al. Metformin suppresses intestinal polyp growth in ApcMin/+ mice. Cancer Sci 2008;99:2136–41.
16. Graham GG, Punt J, Arora M, Day RO, Doogue MP, Duong JK, et al. Clinical pharmacokinetics of metformin. Clin Pharmacokinet 2011;50:81–98.
17. Zhu Z, Jiang W, Thompson MD, McGinley JN, Thompson HJ. Metformin as an energy restriction mimetic agent for breast cancer prevention. J Carcinog 2011;10:17.
18. Dowling RJ, Niraula S, Chang MC, Done SJ, Ennis M, McCready DR, et al. Changes in insulin receptor signaling underlie neoadjuvant metformin administration in breast cancer: A prospective window of opportunity neoadjuvant study. Breast Cancer Res 2015;17:32.
19. Liu X, Romero IL, Litchfield LM, Lengyel E, Locasale JW. Metformin targets central carbon metabolism and reveals mitochondrial requirements in human cancers. Cell Metab 2016;24:728–39.
20. MacLean PS, Giles ED, Johnson GC, McDaniel SM, Fleming-Elder BK, Gilman KA, et al. A surprising link between the energetics of ovariectomy-induced weight gain and mammary tumor progression in obese rats. Obesity (Silver Spring) 2010;18:696–703.
21. Rudolph MC, Wellberg EA, Lewis AS, Terrell KL, Merz AL, Maluf NK, et al. Thyroid hormone responsive protein Spot14 enhances catalysis of fatty acid synthase in lactating mammary epithelium. J Lipid Res 2014;55:1052–65.
22. Wellberg EA, Rudolph MC, Lewis AS, Padilla-Just N, Jedlicka P, Anderson SM. Modulation of tumor fatty acids, through overexpression or loss of thyroid hormone responsive protein spot 14 is associated with altered growth and metastasis. Breast Cancer Res 2014;16:481.
23. Christensen MM, Brasch-Andersen C, Green H, Nielsen F, Damkier P, Beck-Nielsen H, et al. The pharmacogenetics of metformin and its impact on plasma metformin steady-state levels and glycosylated hemoglobin A1c. Pharmacogenet Genomics 2011;21:837–50.
24. Boule NG, Robert C, Bell GJ, Johnson ST, Bell RC, Lewanczuk RZ, et al. Metformin and exercise in type 2 diabetes: Examining treatment modality interactions. Diabetes Care 2011;34:1469–74.
25. Kimura N, Masuda S, Tanihara Y, Ueo H, Okuda M, Katsura T, et al. Metformin is a superior substrate for renal organic cation transporter OCT2 rather than hepatic OCT1. Drug Metab Pharmacokinet 2005;20:379–86.
26. Lettieri Barbato D, Vegliante R, Desideri E, Ciriolo MR. Managing lipid metabolism in proliferating cells: New perspective for metformin usage in cancer therapy. Biochim Biophys Acta 2014;1845:317–24.
27. Poli G, Cantini G, Armignacco R, Fucci R, Santi R, Canu L, et al. Metformin as a new anti-cancer drug in adrenocortical carcinoma. Oncotarget 2016;7:49636–48.
28. Hosono K, Endo H, Takahashi H, Sugiyama M, Uchiyama T, Suzuki K, et al. Metformin suppresses azoxymethane-induced colorectal aberrant crypt foci by activating AMP-activated protein kinase. Mol Carcinog 2010;49:662–71.
29. Kim J, Lee J, Jang SY, Kim C, Choi Y, Kim A. Anticancer effect of metformin on estrogen receptor-positive and tamoxifen-resistant breast cancer cell lines. Oncol Rep 2016;35:2553–60.
30. Pollak M.The insulin and insulin-like growth factor receptor family in neoplasia: an update. Nat Rev Cancer 2012;12:159–69.
31. Stoll BA.Breast cancer and the western diet: Role of fatty acids and antioxidant vitamins. Eur J Cancer 1998;34:1852–6.
32. Chlebowski RT, Blackburn GL, Thomson CA, Nixon DW, Shapiro A, Hoy MK, et al. Dietary fat reduction and breast cancer outcome: Interim efficacy results from the Women's Intervention Nutrition Study. J Natl Cancer Inst 2006;98:1767–76.
33. Sladek CD, Stevens W, Song Z, Johnson GC, MacLean PS. The "metabolic sensor" function of rat supraoptic oxytocin and vasopressin neurons is attenuated during lactation but not in diet-induced obesity. Am J Physiol Regul Integr Comp Physiol 2016;310:R337–45.
34. Cai H, Zhang Y, Han TK, Everett RS, Thakker DR. Cation-selective transporters are critical to the AMPK-mediated antiproliferative effects of metformin in human breast cancer cells. Int J Cancer 2016;138:2281–92.
35. Urakami Y, Okuda M, Saito H, Inui K. Hormonal regulation of organic cation transporter OCT2 expression in rat kidney. FEBS Lett 2000;473:173–6.
36. Takane H, Shikata E, Otsubo K, Higuchi S, Ieiri I. Polymorphism in human organic cation transporters and metformin action. Pharmacogenomics 2008;9:415–22.
37. Kahn BB, Alquier T, Carling D, Hardie DG. AMP-activated protein kinase: Ancient energy gauge provides clues to modern understanding of metabolism. Cell Metab 2005;1:15–25.
38. Morales DR, Morris AD. Metformin in cancer treatment and prevention. Annu Rev Med 2015;66:17–29.
39. Smith TA, Phyu SM. Metformin decouples phospholipid metabolism in breast cancer cells. PLoS One 2016;11:e0151179.
40. Currie E, Schulze A, Zechner R, Walther TC, Farese RV Jr.Cellular fatty acid metabolism and cancer. Cell Metab 2013;18:153–61.
41. Hilvo M, Denkert C, Lehtinen L, Muller B, Brockmoller S, Seppanen-Laakso T, et al. Novel theranostic opportunities offered by characterization of altered membrane lipid metabolism in breast cancer progression. Cancer Res 2011;71:3236–45.
42. Santos CR, Schulze A. Lipid metabolism in cancer. FEBS J 2012;279:2610–23.
43. Corsetto PA, Cremona A, Montorfano G, Jovenitti IE, Orsini F, Arosio P, et al. Chemical-physical changes in cell membrane microdomains of breast cancer cells after omega-3 PUFA incorporation. Cell Biochem Biophys 2012;64:45–59.
44. Chenais B, Blanckaert V. The janus face of lipids in human breast cancer: How polyunsaturated fatty acids affect tumor cell hallmarks. Int J Breast Cancer 2012;2012:712536.
45. Lee EJ, Yun UJ, Koo KH, Sung JY, Shim J, Ye SK, et al. Down-regulation of lipid raft-associated onco-proteins via cholesterol-dependent lipid raft internalization in docosahexaenoic acid-induced apoptosis. Biochim Biophys Acta 2014;1841:190–203.
46. Fabian CJ, Kimler BF, Hursting SD. Omega-3 fatty acids for breast cancer prevention and survivorship. Breast Cancer Res 2015;17:62.
47. Chang NW, Wu CT, Chen DR, Yeh CY, Lin C. High levels of arachidonic acid and peroxisome proliferator-activated receptor-alpha in breast cancer tissues are associated with promoting cancer cell proliferation. J Nutr Biochem 2013;24:274–81.
48. Chung H, Lee YS, Mayoral R, Oh DY, Siu JT, Webster NJ, et al. Omega-3 fatty acids reduce obesity-induced tumor progression independent of GPR120 in a mouse model of postmenopausal breast cancer. Oncogene 2015;34:3504–13.
49. Subedi K, Yu HM, Newell M, Weselake RJ, Meesapyodsuk D, Qiu X, et al. Stearidonic acid-enriched flax oil reduces the growth of human breast cancer in vitro and in vivo. Breast Cancer Res Treat 2015;149:17–29.
50. Niraula S, Dowling RJ, Ennis M, Chang MC, Done SJ, Hood N, et al. Metformin in early breast cancer: A prospective window of opportunity neoadjuvant study. Breast Cancer Res Treat 2012;135:821–30.